Int. J. Electrochem. Sci., 16 **(2021)** Article ID: 210251, doi: 10.20964/2021.02.01

International Journal of
ELECTROCHEMICAL
SCIENCE
www.electrochemsci.org

Study on the Electrochemical Corrosion Behavior of 304 Stainless Steel in Chloride Ion Solutions

Yu Zhang[1], *Changdi Yang*[1], *Lin Zhao*[2,*], *Jiwen Zhang*[1]

[1]School of Mechanical Engineering, Shenyang University, Shenyang 110044, China
[2]Institute of Metal Research, Chinese Academy of Sciences, Shenyang, 110016, China
[*]E-mail: zhaolin@imr.ac.cn

Received: 25 July 2020 / *Accepted:* 24 November 2020 / *Published:* 31 December 2020

The corrosion behavior of 304 stainless steel under different concentrations of Cl^- and specific Fe^{3+} was studied with different immersion times by open-circuit potential, AC impedance, and cyclic voltammetry curves. The results show that with an increase in the concentration of Cl^- in the solution, the stability of 304 stainless steel with the passive film decreased. The potential time curve shows that in the initial stage, the incubation process of pitting can be described by exponential relationship. At the initial stage of immersion, the passive film of austenitic stainless steel hindered the corrosion of Cl^- to some extent, but by prolonging the immersion time, Cl^- destroyed the integrity of the passive film on the surface of austenitic stainless steel, and eventually led to apparent pitting corrosion.

Keywords: 304 stainless steel; passive film; concentration of Cl^-; pitting corrosion

1. INTRODUCTION

304 stainless steel has excellent corrosion resistance and machinability, and hence widely used in petrochemical, shipbuilding, aerospace, and other industrial fields, as an irreplaceable material. Among different types of stainless steel, austenitic stainless steel is extensively used in the industry owing to its relatively low cost, superior corrosion resistance, heat resistance, and mechanical properties, along with good workability and weldability [1,2,3]. The corrosion resistance of 304 stainless steel is much better than that of carbon steel and structural steel in terms of its high performance and low cost. However, with the environment containing Cl^- and other halogen ions, the thick protective film formed by the matrix of 304 and other austenitic stainless steels is quickly damaged. It causes severe pitting corrosion that affects the properties and service life of materials [4,5,6,7]. As pitting corrosion causes failure of the metal materials inadvertently, its destructiveness and danger are much significant than that of uniform corrosion. However, the detection and control of pitting are much more complicated than that

of uniform corrosion. At present, the corrosion behavior of austenitic stainless steel in Cl^- containing environment has demonstrated exciting results [8,9,10,11,12,13,14].

The passive film of austenitic stainless steel formed in the process of corrosion to prevent the further occurrence and development of corrosion [15]. Many researchers [16-18] have set up various theoretical models to describe the growth and breakdown of the passive film. Among them, MacDonald [19,20] proposed a universal passive film growth model- point defect model (PDM) in the early 1980s. The model not only considers the migration of metal cations, oxygen anions and their corresponding vacancies in the passive film but also considers the interaction between them, as well as the cations, anions and related vacancies in the interface of the substrate/passive film and passive film/solution. Also, to describe the growth of passive films, the point defect model (PDM) was used to explain the breakdown of passive films and the effect of elements on passive films. This study also refers to the theory to analyze the failure process of the passive film in the corrosion process [21,22].

The effect of Cl^- on the passive film and pitting is particularly serious in the long-term service. Yang [6] measured pitting potential in the corrosion process by the potentiodynamic polarization method. It has been found that with an increase in temperature and concentration of Cl^-, the breakdown potential Eb of 304 stainless steel shifted negatively, and the size and number of pits were increased. The corrosion behavior of 304 stainless steel in dilute hydrochloric acid was studied by Ju [13], and it has been noted that the pitting corrosion sensitivity of 304 stainless steel increased with an increase in the concentration of chloride ion. At the same time, with an increase in time, the corrosion accelerated. Li[14] studied the local corrosion of 304 stainless steel with electrochemical noise. The corrosion process divided into four stages: the passive stage, metastable pitting stage, steady pitting stage, and late steady pitting stage. The above research focused on the process of pitting and sensitivity of pitting due to changes in the external environment. However, the corrosion of stainless steel is a long-term process, and researches on such a long-term corrosion process are relatively rare, as well as the whole corrosion behavior of 304 stainless steel has not been explored in depth.

The oxidation characteristics of Fe^{3+} can promote the formation of the passive film in the matrix and accelerate the destruction process of the passive film by chloride ion. On the other hand, the corrosivity characteristics of Fe^{3+} can corrode the matrix.

In this study, a specific concentration of Fe3+ was set to accelerate the formation of the passive film, and then we analyzed the destructive effect of different chloride ion concentration on the passive film, during which the Fe3+ concentration was reduced as far as possible to prevent obvious corrosion effect on the substrate.

In this study, open-circuit potential, cyclic voltammetry curve, and electrochemical impedance spectroscopy were used to study the effect of concentration of Cl^- and immersion time on the corrosion behavior of 304 stainless steel at a specific concentration of Fe^{3+}.

2. EXPERIMENTAL METHODS

2.1 Experimental Materials

For the experiments, 304 austenitic stainless steel sheet with the thickness in 3mm was used. Its chemical composition is C 0.055, Si 0.44, Mn 1.21, S 0.003, Cr 18.28, Ni 8.13 with marginal Fe. 304 austenitic stainless steel sheet was cut into square specimens of 10 mm × 10 mm × 3 mm.

After soldering copper wires on the non-working surface by the tin welding method, the non-working surface was encapsulated using epoxy resin, and a 10 mm x 10 mm electrode working surface was reserved. After curing with epoxy resin, we wiped it with alcohol and acetone, cleaned with distilled water, and kept in a dryer for the electrochemical test. All the employed reagents such as $FeCl_3.6H_2O$ for the experiments were of analytical grade, and the solution was prepared using deionized water. FeCl3 solution is prepared according to ASTM g48-11" Standard Test Methods for Pitting and Crevice Corrosion Resistance of Stainless Steels and Related Alloys by Use of Ferric Chloride Solution". The Cl^- concentration can be adjusted by adding the corresponding concentration of NaCl, and the specific concentration of Fe^{3+} is 1.0×10^{-3} mol/L.

2.2 Electrochemical measurement

For the electrochemical tests, CS350 electrochemical workstation was used, and measurements were made using the standard three-electrode system: the working electrode was 304 stainless steel, Pt electrode was used as an auxiliary electrode; the reference electrode consisted of a salt bridge and saturated calomel electrode(SCE).

The open-circuit potential-time curve of the system was measured at a sampling frequency of 5Hz and recorded for 48h. The cyclic voltammetry curve was used to test the 304 stainless steel working electrode. The scanning range of the cyclic polarization test was -0.8 V ~ + 2.0 V relative to open-circuit potential. The scanning rate was 5 mV/s. When the anodic polarization current density was more than 1 mA/cm^2, the reverse scanning was performed immediately. The amplitude of the sinusoidal AC signal applied by the electrochemical impedance spectroscopy (EIS) test was 5 mV, and the scanning frequency was ranging from 10^5 to10^{-2} Hz. The impedance spectra obtained by the EIS test were fitted by the Zview software.

After different times (1, 12, 24, 48 h) of immersion in the solution, the 304 samples were rinsed with deionized water and dried with hot wind. The corrosion morphology was tested by Hitachi s4800 scanning electron microscope (SEM).

3. EXPERIMENTS AND DISCUSSION

3.1 Open-circuit potential-time curve (OCP) results

The open-circuit potential-time curve (EOCP-t) of 304 stainless steel was monitored for 48 h by immersing in a solution of 1.0×10^{-3} mol/L Fe^{3+} and 3.0×10^{-3}, 3.0×10^{-2}, 1.0×10^{-1}, 2.0×10^{-1} mol/L Cl^-. From the figure1 (a), it could be noted that the open-circuit potential in the above solution system has the same trend with time. The values of EOCP increase rapidly at the beginning of immersion, indicating

that the surface of the electrodes changes. At this time, the passivation of stainless steel under the action of trivalent ions of ferric oxide should occur, resulting in the formation of a dense oxide film on the surface, which in turn leads to a rapid increase in the potential.

After immersing for an hour, the EOCP value increased slowly but still maintained an upward trend. At this time, the passive film on the electrode surface began to grow slowly and stabilized gradually. Then, with the gradual stabilization of the passivation film, the destruction and dynamic equilibrium of the passivation film occur on the surface of the electrode. Thus, the value was stable within a certain range without any apparent fluctuation. After the later stage of immersion, the value decreased slowly owing to the destructive reaction of chloride ions to the passive film covered by the surface of the electrode, resulting in the breakdown of the passive film and a decrease in the EOCP value.

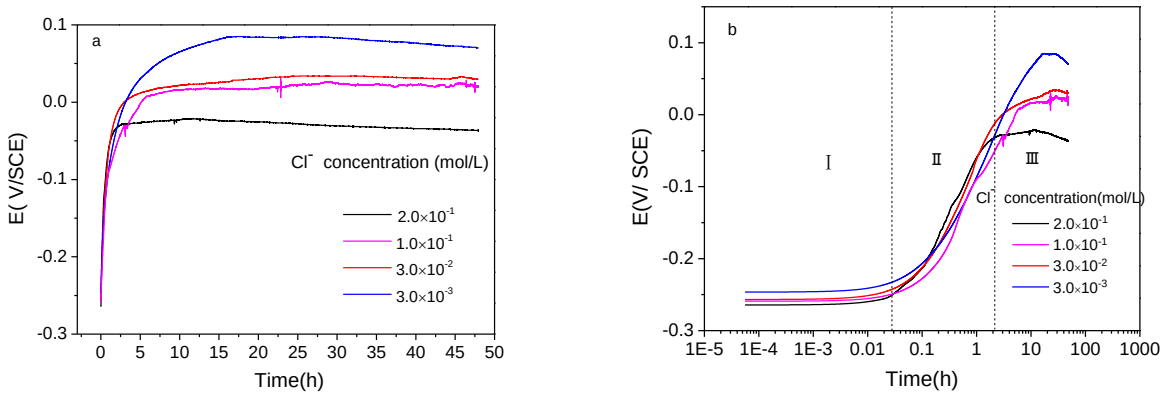

Figure 1. EOCP-time curves of 304 stainless steel in solutions with different concentrations of Cl^- (a: normal coordinate curve; b: logarithm of x-axis time)

Therefore, the potential-time curve (EOCP-t) of 304 stainless steel in solutions of different chloride concentrations can be divided into three stages based on the changes in the potential, as shown in Figure (b). The first stage is the formation of the passive film, where the potential rises rapidly, corresponding to phase I in the figure, the time for different Cl^- concentration is about 2 minutes from the beginning; the second stage is the dynamic stability, where the potential is continuously rising slowly, corresponding to phase II in the figure. At this stage, the time of different concentrations was different, and the high concentration of chloride ions entered the third stage earlier; and the third stage is the destruction of the passive film, corresponding to phase III in the figure, where chloride ions begin to destroy the passive film slowly. The open-circuit potential decreases with time when 304 stainless steel matrix corrodes.

From the comparison of open-circuit potential-time curves, it can be seen that the presence of chloride ions has a significant influence on the formation of passive films. In the system with a Cl^- concentration of 3.0×10^{-3} mol/L, the EOCP value did not show a significant transition, and the increase was relatively stable. The transition did not occur until about 16 h, and it entered into the third stage. In the system with a Cl^- concentration of 0.1 mol/L, the EOCP value changed in about 3 h and began to enter into the third stage.

In the stages I and II, it is the process of pitting initiation and propagation. The potential time curve can be approximately described by an exponential relationship [23]:

$$E = e^{At} \quad (1)$$

Where *E* is the open circuit potential, *t* is the measurement time, and *A* is the coefficient, which is determined by chloride concentration and other factors.

According to PDM model, the rapid increase of potential is the formation of passive film in the initial stage; then in the second stage, the growth and dissolution of passive film are in dynamic equilibrium after forming a complete passive film on the metal surface. The continuous oxidation of metal at the film/metal interface leads to the growth of passive film, and the dissolution of metal cations in the film/solution interface will lead to the continuous dissolution of the passive film by itself. In general, the two processes are the state of dynamic equilibrium, and the thickness of passive film has a linear relationship with potential and pH. When the migration velocity of metal vacancy to metal/film interface (or the formation speed of metal atom vacancy) is greater than the immersion velocity of metal atom vacancy into metal, the metal atom vacancy will accumulate at the metal/film interface and form a metal hole under the passive film. When the size of metal hole exceeds the critical value, the passivation film will rupture. The time from the formation of metal hole to the critical size is the induction time of pitting, which is the second stage.

After that, the open circuit potential began to decrease with the breakdown of passive film and the migration of chloride ion. However, it is obviously different that the destruction of passivation film by different concentration of chloride ion. Under the stable state of open circuit potential, the stable open circuit potential values of each concentration decreased with an increase in the concentration of chloride ion. After 48 h of immersion, the open circuit potential values changed significantly. The EOCP value is 0.07 V in 3.0×10^{-3} mol/L solution and -0.0366 V in a 0.2 mol/L solution, indicating that chloride ion can significantly reduce the open-circuit potential of 304 stainless steel in a stable state.

3.2 Cyclic voltammetry curves results

The cyclic voltammetry curves of the samples were measured after soaking for 1 h and 12 h. As shown in Fig. 2, the corresponding characteristic parameters are listed in Table 1. The cyclic voltammetry curves show the same regularity at different concentrations. In the forward sweep process, when the test potential was higher than the self-corrosion potential, the anode current of the electrode increased rapidly with an increase in potential. When the anode current increased to an absolute value, it began to decrease with an increase in the potential, showing an apparent S-shaped transition. It then entered into the passivation region, and at this time, the potential increased while the current density remained stable. When the potential continued to rise, it began to enter the pitting area, and apparent pitting rings appeared, which was the characteristic of pitting corrosion on the surface of the electrode [24, 25].

In the cyclic voltammetry curve, when the potential and current begin to rise reciprocal, the potential is the pitting potential, Eb. After the pitting ring closes, the potential becomes stable, while the current decreases. At this time, the potential is the dimensionally passive potential, Ep. Among them,

the more negative the Eb value of the stainless steel pitting corrosion, the more quickly the pitting corrosion occurs, and the corrosion resistance of the material significantly reduced. In the front of the pitting ring in the cyclic voltammetry curve, the current fluctuates, demonstrating the presence of metastable pitting holes, i.e., the local dissolution and re-passivation of the passive film on the surface of stainless steel [26, 27].

Combining with the parameters of cyclic voltammetry curve, it has been found that l Eb of 3.0 $\times 10^{-3}$ mol/L Cl^- solution is the largest than others, and its resistance to pitting is the best when immersed for 1 h, indicating that the ability of Cl^- to destroy the passive film is weak at low concentrations. While the corrosive potential Ecorr is lower, and the value of Eb-EP is maximum at a concentration of 0.1 mol/L compared to other concentrations, which is consistent with the results of Eocp. Therefore, Eb value is relatively high at this concentration, indicating a threshold concentration for chloride when immersed for 1 h. Around this range of concentration, the passive film is quickly destroyed, but at the same time, the ability to repair the passive film is stronger.

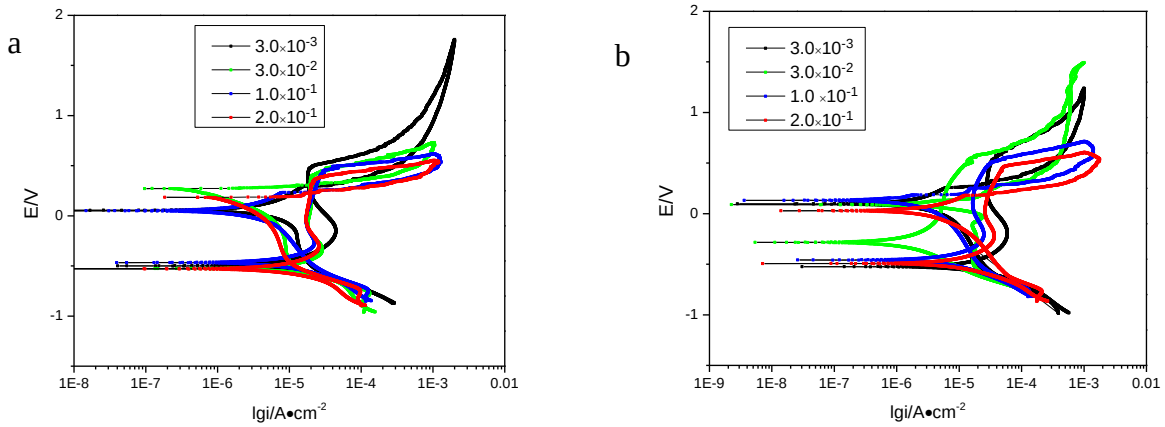

Figure 2. a. Cyclic voltammetry curves of 304 stainless steel in solutions of different concentrations of Cl^- after 1 h and 12 h

Table 1. Characteristic values on the cyclic voltammetry curves of 304 stainless steel at different concentrations of Cl^- after 1 h and 12 h

C Cl^-/ mol/L	E_{corr} / V		**E_b / V**		E_p / V		E_b-E_p / V	
	1 h	12h	1 h	12 h	1 h	12 h	1h	12 h
3.0×10^{-3}	-0.499	-0.524	-0.463	-0.528	-0.292	-0.279	0.170	0.250
3.0×10^{-2}	-0.527	-0.283	-0.396	-0.497	-0.305	-0.131	0.091	0.367
1.0×10^{-1}	-0.467	-0.459	-0.456	-0.500	-0.231	-0.248	0.225	0.252
2.0×10^{-1}	-0.529	-0.493	-0.346	-0.463	-0.218	-0.181	0.128	0.282

After 12 h of immersion, the pitting breakdown potential Eb in Cl^- solution of 3.0 $\times 10^{-3}$ mol/L is the largest, while in Cl^- solution of 0.2 mol/L is the smallest. It also shows that the effect of damage on the passive film is proportional to the concentration of Cl^-. The maximum value of EP is 3.0 $\times 10^{-3}$ mol/L, and that of Eb-EP is 3.0 $\times 10^{-2}$ mol/L, which is different from the case of 1 h. This shows that the higher the concentration of Cl^- along with prolonging the time, the more obvious the damage to the passive film

on the surface of the material, and it is more difficult to repair the passive film with an increase in the concentration of Cl^-.

Based on the above analysis, the concentration of Cl^- in the solution has a remarkable influence on the corrosion behavior of 304 stainless steel. With an increase in the concentration of Cl^-, the damage to the passive film on the surface of the electrodes increases, the stability of the passive film becomes worse, the passivation interval decreases, and the pitting corrosion resistance of the stainless steel decreases.

According to PDM theory [19, 20], with an increase in the concentration of Cl^- in the solution, there is competitive adsorption between Cl^- and anions formed by the passive film. The adsorption of Cl^- makes the cationic vacancies at the membrane/solution interface to be replaced by Cl^- easily and the probability of metal oxides turning into soluble chlorides increases, which has a stronger destructive effect on the passive film. Therefore, with an increase in the concentration of Cl^-, the passive film on the surface of the electrode is prone to local corrosion.

As an example, the polarization curve was measured in a solution of Fe^{3+} (3.0×10^{-3} mol/L) + Cl^- (3.0×10^{-3} mol/L), and the effects of chloride ions on the electrodes at different stages were studied. Fig. 3 shows the cyclic voltammetry curves of 304 stainless steel electrodes immersed in 1.0×10^{-3}mol/L of Fe^{3+} and 3.0×10^{-3} mol/L of Cl^- solution at different times. The characteristic parameters are shown in Table 2. It can be seen from figure 2 that the polarization curves at different times generally agree, with apparent pitting rings. With prolonging the corrosion time, the cathodic polarization curve demonstrates the same trend, and the anodic polarization curve shows a significant difference.

The higher Eb values at the initial stage of immersion indicated that the passive film played a prominent role in inhibiting the pitting corrosion. Eb values began to decrease significantly after 12 h, and the protective effect of passive film weakened by the action of Cl^- for a long time, which made it easier to break down.

With the continuation of immersion time, the values of Ecorr and Eb shifted negatively, indicating that the pitting corrosion of the electrodes became more prone, and stability of the passive film decreased with an increase in the immersion time. The value of Eb-Ep increases with an increase in the immersion time, indicating that pitting corrosion occurs quickly on the electrode surface, and the self-repairing ability of passive film decreases.

According to the theory of passivation film rupture [28], the Mechanical forces formed by electrostrictive or surface tension caused the localized rupture of passive film at weak sites and defects. In a non aggressive medium, the local rupture of the passive film will be repaired quickly. In fact, the anode current is the statistical sum of the transient current from a large number of rupture and repair events of the passive film.

However, in the corrosive solution containing chloride ion in this experiment, with the prolongation of immersion time, the tendency of the passive film to be repaired is greatly reduced, and the passive film will be completely broken. The chloride ion reacts with metal to form chloride after migrating to the passive film/metal interface, the pressure caused by chloride accumulation will lead to the rupture of passive film, and chloride ion produced by chloride dissolution can stabilize the initial growth of pitting corrosion, which leads to the initiation of pitting corrosion. The increase of chloride concentration also accelerates the process.

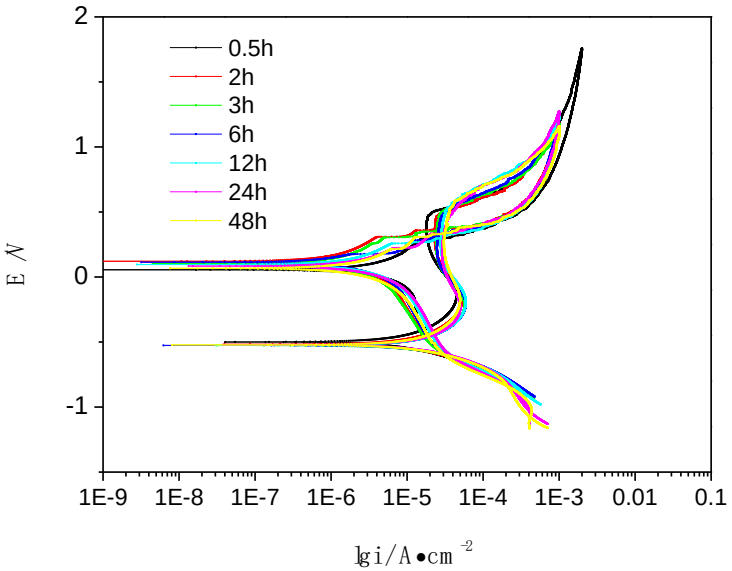

Figure 3. Cyclic voltammetry curves of 304 stainless steel in a solution of Cl^- (3.0×10^{-3}mol/L) at different times (0.5, 2, 3, 6, 12, 24, 48 h)

Table 2. Characteristic parameters of cyclic voltammetry curve of stainless steel immersed in a solution of Fe^{3+} (1.0×10^{-3} mol/L) + Cl^- (2.0×10^{-1} mol/L) at different times

Time/h	E_{corr}/V	E_b/V	E_p/V	E_b-E_p/V
1	-0.500	0.446	0.287	0.158
2	-0.518	0.454	0.358	0.096
3	-0.527	0.440	0.342	0.098
6	-0.526	0.401	0.271	0.130
12	-0.525	0.434	0.320	0.114
24	-0.521	0.323	0.303	0.021
48	-0.522	0.333	0.302	0.030

3.3 EIS results

Fig. 4 is the EIS diagram of 304 stainless steel electrodes immersed in a solution of 1.0×10^{-3} mol/L Fe^{3+} and 3.0×10^{-3} mol/L of Cl^- for different times. Fig. 5 is the equivalent circuit diagram. The fitted electrochemical parameters are listed in Table 2. Among them, R_S is the solution resistance, Rct is the charge transfer resistance, CPE is the constant phase angle element which is composed of double-layer capacitance CPE-T and dispersion coefficient CPE-P. The dispersion coefficient can reflect the density of passivation film so that the dispersion effect of the ideal smooth planar electrode is 1. From the Nyquist diagram, it can be seen that the impedance spectrum is a single capacitive arc resistance semicircle, showing the characteristics of capacitive reactance. From the trends in the capacitive arc resistance, it can be found that the radius of capacitive arc resistance increases gradually in the initial 12 h, and then decreases gradually, showing the regularity. This indicates that the passive film has a certain hindrance effect on pitting corrosion in the initial stage.

With an increase in time, the destructive effect of Cl^- on passive film increases gradually, and the corrosion begins seriously. From the electrochemical parameters of impedance, as shown in Table 2, it can be found that the capacitive arc radius increases at the beginning of immersion, and the Rct value reaches its maximum at 12 h, confirming that the passivation film of the electrode is compact and Cl^- is difficult to break through the passivation film to reach the substrate within 12 h. At this time, the stainless steel is in the passivation state with excellent corrosion resistance and pitting corrosion does not occur, which is consistent with the law of open circuit potential change. By extending immersion, the solution resistance Rs decreases, and the RCT value at 48 h is about two times smaller compared to 1 h. The impedance Z and phase angle decrease gradually, and the corresponding peak of the phase angle narrows gradually. This denotes that with an increase in the immersion time, the stability of the passive film decreases, and the corrosion resistance decreases. After 12 h, CPE-T increases gradually, and CPE-P decreases, implying that the diffusion effect of ions in solution increases and the ability of diffusion increases. Cl^- easily reaches and adsorbs on the surface of passive film or surface vacancies, leading to an increase in the cationic vacancies at the membrane/metal interface and the concentration of cationic vacancies. It leads to the acceleration of the dissolution rate of the passive film, more vacancies of the passive film, and easier formation and development of pitting [29, 30].

Combined with the previous experimental results, after 12 h, the passive film ruptured and the polarization curve showed a rapid current transition near Eb. This process is the transformation process from metastable pitting to steady pitting. The difference between metastable pitting and steady pitting is the size of pits. Metastable pitting cannot maintain the corrosiveness of internal solution by the depth of pits itself, so additional diffusion barriers are needed to maintain the corrosivity of the solution inside the pit. Correspondingly, the steady pitting is that when the pit grows to a certain size (the critical size of metastable/steady pitting); its depth is enough to maintain the corrosivity of the internal solution. At this time, whether the residual passivation film of the pit is broken or not, pitting can still maintain stable growth.

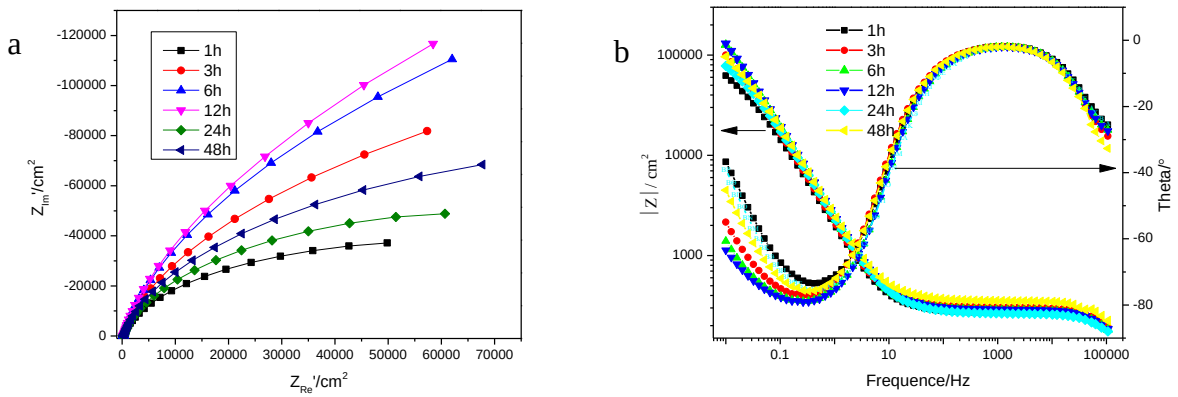

Figure 4. EIS diagrams of 304 stainless steel immersed in Fe^{3+} (1.0×10^{-3} mol/L) and Cl^- (1.0×10^{-3} mol/L) solution at different times(a, Nyquist; b, bode)

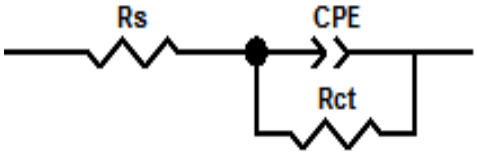

Figure 5. Equivalent circuit diagram

Table 3. Electrochemical parameters of the immersed 304 stainless steel at different times (1h,3h,6h,12h,24h,48h)by the fitting of electrochemical impedance spectroscopy

Time/h	Rs/ Ω .cm^2	R_{ct}/ Ω .cm^2	CPE-T/ μ F·cm^{-2}	CPE-P
1	18.32	87184	113.47	0.8324
3	20.56	87534	119.22	0.8432
6	20.75	89345	106.84	0.8557
12	21.64	90346	118.24	0.8776
24	19.81	52477	119.35	0.8548
48	17.89	43562	122.73	0.8212

Scanning electron microscopy results also prove this point further. Fig. 6 shows the scanning electron microscopy images at different immersion times. In the first 12 h, only slight pitting marks on the surface could be noted. After 12 h, distinct pits appear on the surface. At 48 h, large corrosion marks could be observed. The surface topographic photographs show that pits on the surface have undergone the process of occurrence, development, and growth with extending the immersion time gradually, and the transition from metastable to steady pitting.

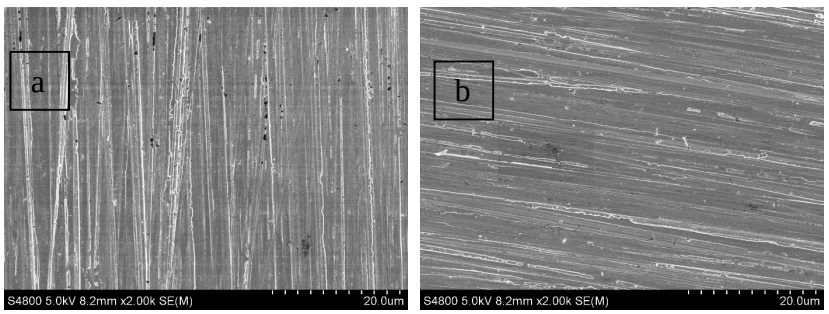

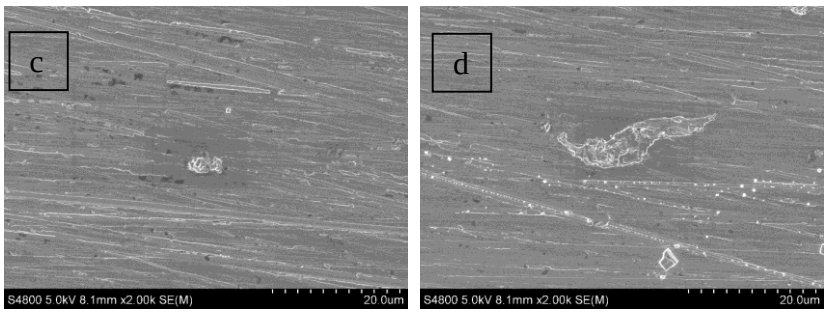

Figure 6. Scanning electron microscopic photographs at different immersion times (a:1h, b:12 h, c:24 h, d:48h)

4. CONCLUSIONS

(1) With an increase in the concentration of Cl^- in the solution, the stability of passive film of 304 stainless steel decreases, and the pitting corrosion resistance decreases. The potential time curve shows that in the initial stage, the incubation process of pitting can be described by exponential relationship.

(2) In the initial stage of immersion, the passivation film of austenitic stainless steel can hinder the corrosion of Cl^- to some extent, but with the prolongation of immersion time, Cl^- destroys the integrity of the passivation film on the surface of austenitic stainless steel, and eventually leading to apparent pitting corrosion.

ACKNOWLEDGMENTS
This work was partially supported by Science and technology program of Liaoning Province (20170540637).

References

1. I. O. Wallinder, J. Lu, S. Bertling, and C. Leygraf, *Corros. Sci.*, 44 (2002) 2303.
2. S. Zhang, Z. Jiang, H. Li, H. Feng, B. Zhang, *J. Alloys Compd.,* 695 (2017) 3083.
3. J. Li, B. Deng, Y. M. Jiang. *Corrosion & Protection*, 30 (2009) 595.
4. K. M. Deen, M.A. Virk, C.I. Haque, I.H. Khan, *Eng. Fail. Anal*., 17 (2010) 886.
5. S.H. Kim, J.H. Lee, J.G. Kim, *Met. Mater. Int*., 24 (2018) 516.
6. R. C. Yang, H. J. Bi, S. R. Niu. *Journal of Lanzhou University of Technology*, 36 (2010) 5.
7. A. Gagliardi, A. Lanzutti, M. Simonato, R. Furlanetto, M. Magnan, F. Andreatta, L. Fedrizzi, *Eng. Fail. Anal.*, 92 (2018) 289.
8. S.S. Qian, Y. Y. Liu, L. Q. Yin, X. Wu, J. Li, J. M. Wang, F. Lyu, Y. M. Jiang.*J. Electrochem. Soc.,* 167 (2020) 021506.
9. C. O. A. Olsson, D. Landolt. *Electrochim. Acta*, 48 (2003) 1093.
10. O. M. Alyousif, R. Nishimura. *Corros. Sci*., 49 (2007) 3040.
11. S. Cho, J.H. An, S. H. Lee, J. G. Kim*, Int. J. Electrochem. Sci.,* 15 (2020) 4406.
12. D. M. Sun, Y. M. Jiang, Y. Tang. *Electrochim. Acta,* 54 (2009) 1558.
13. Y. Ju, W. D. Zhu, P. C. Wang. *Hot Working Technology*, 43 (2014) 53.
14. J. Li, L. Zhao, B. W. Li. *Chin. Soc. Corros. Prot.,* 32 (2012) 235.
15. J.W. Schultze, M. M. Lohrengel. *Electrochim. Acta*, 45 (2000) 2499.
16. N. Cabrera, N.F. Mott. *Rep.Prog.Phys*., 12 (1948) 163.

17. F.P. Fehlner, N.F. Mott. *Oxid. Met.,* 2 (1970) 59.
18. E.J.W. Verwey. *Phys 2.,* (1935) 1059.
19. D. D. Macdonald. *Electrochim. Acta*, 56 (2011) 1761.
20. D. D. Macdonald. *J. Electrochem. Soc*., 139 (1992) 3434.
21. M. S. Qurashi, Y. Cui, J. Wang, N. Dong, J. Bai, Y. Wu, P. Han. *Int. J. Electrochem. Sci.,* 14 (2019) 10642.
22. N.B. Hakiki, S. Boudin, B. Rondot, M. Da Cunha Belo. *Corros. Sci*., 37 (1995) 1809.
23. L. F. Lin, C. Y. Chao, D. D. Macdonald. *J. Electrochem. Soc*., 128 (1981) 1194.
24. C. G. Wang, J. H. Dong, W. Ke. *Acta Mech. Sin*., 48 (2012) 85.
25. M. C. Li, C. L. Zeng. *Corrosion Science and Protection Technology*, 14 (2002) 132.
26. P. E. Manning, D. J. Duquette. *Corros. Sci.,* 48 (2011) 597.
27. A. Turnbull, M. Ryan, A. Willetts. *Corros. Sci.,* 45 (2008) 1051.
28. G.S. Frankel. *J. Electrochem. Soc*., 145 (1998) 2186
29. M. C. Li, C. L. Zen, S. Z. Lou, J. N. Shen, H. C. Lin, C. N. Cao. *Electrochim. Acta*, 48 (2003) 1735.
30. M. C. Li, L. L. Jiang, W. Q. Zhang, Y. H. Qian, S. Z. Luo, J. N. Shen. *J. Solid State Electrochem.,* 11 (2007) 1319.